

# Polarization effects in tau production by neutrino\*

K. Hagiwara<sup>a</sup>, K. Mawatari<sup>b†</sup> and H. Yokoya<sup>cd‡</sup>

<sup>a</sup>Theory Group, KEK, Tsukuba 305-0801, Japan

<sup>b</sup>Graduate School of Science and Technology, Kobe University, Nada, Kobe 657-8501, Japan

<sup>c</sup>Department of Physics, Hiroshima University, Higashi-Hiroshima 739-8526, Japan

<sup>d</sup>Radiation Laboratory, RIKEN, Wako 351-0198, Japan

We studied polarization effects in tau production by neutrino-nucleon scattering. Quasi-elastic scattering,  $\Delta$  resonance production and deep inelastic scattering processes are taken into account for the CERN-to-Gran Sasso projects. We show that the tau produced by neutrino has high degree of polarization, and its spin direction depends non-trivially on the energy and the scattering angle of tau in the laboratory frame.

## 1. INTRODUCTION

In the forthcoming neutrino experiments,  $\nu_\tau$  appearance which is the positive evidence of  $\nu_\mu \rightarrow \nu_\tau$  oscillation is the one of main subjects, as well as precise measurements of neutrino oscillation parameters and unknown  $\theta_{13}$  or CP phase measurement. In 2005, ICARUS [1] and OPERA [2] experiments using the CNGS beam [3] will start to detect  $\nu_\tau$  appearance.

$\nu_\tau$  should be detected through the  $\tau$  production by charged current reactions off a nucleon target. As we pointed out in the recent paper [4], the information on the spin polarization of  $\tau$  produced by neutrino is essential to determine the  $\tau$  production signal since the decay particle distributions depend crucially on the  $\tau$  polarization.

We present polarization effects in  $\tau$  production by neutrino-nucleon scattering via charged current. We consider Quasi-elastic scattering (QE),  $\Delta$  resonance production (RES) and deep inelastic scattering (DIS) processes, which give dominant contributions in the CNGS beam energy region, in the laboratory frame [5].

\*presented by K. Mawatari in oral session and by H. Yokoya in poster session at the 3rd International Workshop on Neutrino-Nucleus Interactions in the Few GeV Region (NuInt04), March 17-21, 2004, Gran Sasso, Italy.

†email address: mawatari@radix.h.kobe-u.ac.jp

‡email address: yokoya@theo.phys.sci.hiroshima-u.ac.jp

## 2. KINEMATICS AND FORMALISM

We show the physical regions of kinematical variables and give the relation between the  $\tau$  spin polarization vector and the spin density matrix of the charged current  $\tau$  production process. In this report, we take account of only  $\tau^-$  production. You can find more details in Ref. [4].

### 2.1. Kinematical region for each process

We consider  $\tau^-$  production for each process by neutrino off a nucleon target in the laboratory frame;

$$\nu_\tau(k) + N(p) \rightarrow \tau^-(k') + \begin{cases} N'(p') & (\text{QE}) \\ \Delta(p') & (\text{RES}) \\ X(p') & (\text{DIS}) \end{cases} \quad (1)$$

The four-momenta are

$$\begin{aligned} k &= (E_\nu, 0, 0, E_\nu), \\ p &= (M, 0, 0, 0), \\ k' &= (E_\tau, p_\tau \sin \theta, 0, p_\tau \cos \theta), \end{aligned} \quad (2)$$

and Lorentz invariant variables are defined as

$$Q^2 = -q^2, \quad q = k - k', \quad (3)$$

$$W^2 = (p + q)^2. \quad (4)$$

Each process is distinguished by the hadronic invariant mass  $W$ :  $W = M$  for QE, and  $M + m_\pi <$

$W < W_{\text{cut}}$  for RES.  $W_{\text{cut}}$  is an artificial boundary between the RES and DIS ( $W > W_{\text{cut}}$ ) processes<sup>1</sup>, and we take  $W_{\text{cut}} = 1.6$  GeV.

Figure 1 shows the kinematical region of each QE, RES and DIS process on the  $(p_\tau \cos \theta, p_\tau \sin \theta)$  plane at  $E_\nu = 10$  GeV.

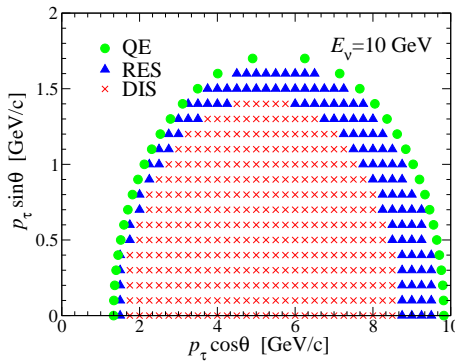


Figure 1. Physical region at  $E_\nu = 10$  GeV

## 2.2. Spin polarization vector of $\tau$

The spin polarization vector of  $\tau$  is defined as

$$\vec{s} = \frac{P}{2}(\sin \theta_P \cos \varphi_P, \sin \theta_P \sin \varphi_P, \cos \theta_P) \quad (5)$$

in the  $\tau$  rest frame in which the z-axis is taken along its momentum direction in the laboratory frame.  $P$  denotes the degree of polarization.  $P = 1$  gives the fully polarized  $\tau$ , and  $P = 0$  gives unpolarized  $\tau$ . The degree of polarization ( $P$ ) and the spin directions ( $\theta_P, \varphi_P$ ) are functions of the tau energy  $E_\tau$  and the scattering angle  $\theta$ .

This spin polarization vector is related to the spin density matrix  $R_{\lambda\lambda'}$ :

$$\frac{dR_{\lambda\lambda'}}{dE_\tau d\cos \theta} = \left(\frac{1}{2} + \vec{s} \cdot \vec{\sigma}\right) \frac{d\sigma_{\text{sum}}}{dE_\tau d\cos \theta}. \quad (6)$$

The spin density matrix is calculated as  $R_{\lambda\lambda'} \propto M_\lambda M_{\lambda'}^*$ , where  $M_\lambda$  is the helicity amplitude with the  $\tau$  helicity  $\lambda/2$  defined in the laboratory frame,

<sup>1</sup>In Ref. [6], the modifications to the PDF's [7] are considered.

and  $d\sigma_{\text{sum}} = dR_{++} + dR_{--}$  is the usual spin summed cross section.

The spin density matrix of  $\tau$  production is obtained by using the leptonic and hadronic tensor as

$$\frac{dR_{\lambda\lambda'}}{dE_\tau d\cos \theta} = \frac{G_F^2 \kappa^2}{4\pi} \frac{p_\tau}{ME_\nu} L_{\lambda\lambda'}^{\mu\nu} W_{\mu\nu}, \quad (7)$$

where  $G_F$  is Fermi constant and  $\kappa = M_W^2/(Q^2 + M_W^2)$ . The leptonic tensor is expressed as

$$L_{\lambda\lambda'}^{\mu\nu} = j_\lambda^\mu j_{\lambda'}^\nu {}^*, \quad (8)$$

where the leptonic weak current  $j_\lambda^\mu$  is

$$j_\lambda^\mu = \bar{u}_\tau(k', \lambda) \gamma^\mu \frac{1 - \gamma_5}{2} u_\nu(k). \quad (9)$$

## 3. HADRONIC TENSORS

We show the hadronic tensors which we used in our calculation for each process, i.e., QE, RES and DIS. Several parameters and form factors were updated to the recent our paper [4].

### 3.1. Quasi-elastic scattering (QE)

The hadronic tensor for the QE scattering process;

$$\nu_\tau + n \rightarrow \tau^- + p \quad (10)$$

is written by using the hadronic weak transition current  $J_\mu$  as follows [8]:

$$W_{\mu\nu}^{\text{QE}} = \frac{\cos^2 \theta_c}{4} \sum_{\text{spins}} J_\mu J_\nu {}^* \delta(W^2 - M^2), \quad (11)$$

where  $\theta_c$  is the Cabibbo angle.  $J_\mu$  are defined as

$$J_\mu = \bar{u}_p(p') \Gamma_\mu u_n(p), \quad (12)$$

where  $\Gamma_\mu$  is written in terms of the six weak form factors of the nucleon,  $F_{1,2,3}^V$ ,  $F_A$ ,  $F_3^A$  and  $F_p$ , as

$$\begin{aligned} \Gamma_\mu = & \gamma_\mu F_1^V + \frac{i\sigma_{\mu\alpha} q^\alpha \xi}{2M} F_2^V + \frac{q_\mu}{M} F_3^V \\ & + \left[ \gamma_\mu F_A + \frac{(p + p')_\mu}{M} F_3^A + \frac{q_\mu}{M} F_p \right] \gamma_5. \end{aligned} \quad (13)$$

We can drop  $F_3^V$  and  $F_3^A$  because of time reversal invariance and isospin symmetry. Moreover, the vector form factors  $F_1^V$  and  $F_2^V$  are related

to the electromagnetic form factors of nucleons under the conserved vector current hypothesis:

$$\begin{aligned} F_1^V(q^2) &= \frac{G_E^V - \frac{q^2}{4M^2}G_M^V}{1 - \frac{q^2}{4M^2}}, \\ \xi F_2^V(q^2) &= \frac{G_M^V - G_E^V}{1 - \frac{q^2}{4M^2}}, \end{aligned} \quad (14)$$

where

$$G_E^V = \frac{1}{(1 - q^2/M_V^2)^2}, \quad G_M^V = \frac{1 + \xi}{(1 - q^2/M_V^2)^2}, \quad (15)$$

with a vector mass  $M_V = 0.84$  GeV and  $\xi = 3.706$ . For the axial form factor  $F_A$  and  $F_p$ , we use:

$$F_A(q^2) = \frac{F_A(0)}{(1 - q^2/M_A^2)^2}, \quad (16)$$

$$F_p(q^2) = \frac{2M^2}{m_\pi^2 - q^2} F_A(q^2), \quad (17)$$

with  $F_A(0) = -1.27$  [9] and an axial vector mass  $M_A = 1.026$  GeV [10]. Notice that the pseudoscalar form factor  $F_p$  plays an important role for the polarization of  $\tau$  produced by neutrino because its contribution is proportional to the lepton mass and it has the spin-flip nature, although it is not known well. In Ref. [11], we discussed it in detail.

### 3.2. Resonance production (RES)

The hadronic tensor for the  $\Delta$  resonance production (RES) process;

$$\nu_\tau + n(p) \rightarrow \tau^- + \Delta^+ (\Delta^{++}) \quad (18)$$

is calculated in terms of the nucleon- $\Delta$  weak transition current  $J_\mu$  as follows [8,12,13]:

$$W_{\mu\nu}^{\text{RES}} = \frac{\cos^2 \theta_c}{4} \sum_{\text{spins}} J_\mu J_\nu^* |f(W)|^2, \quad (19)$$

where  $f(W)$  is the Breit-Wigner factor

$$f(W) = \frac{\sqrt{W\Gamma(W)/\pi}}{W^2 - M_\Delta^2 + iW\Gamma(W)} \quad (20)$$

with its running width

$$\Gamma(W) = \Gamma(M_\Delta) \frac{M_\Delta}{W} \frac{\lambda^{\frac{1}{2}}(W^2, M^2, m_\pi^2)}{\lambda^{\frac{1}{2}}(M_\Delta^2, M^2, m_\pi^2)}. \quad (21)$$

$\Gamma(M_\Delta) = 0.12$  GeV and  $\lambda(a, b, c) = a^2 + b^2 + c^2 - 2(ab + bc + ca)$ . The current  $J_\mu$  for the process  $\nu_\tau + n \rightarrow \tau^- + \Delta^+$  is defined by

$$J_\mu = \langle \Delta^+(p') | \hat{J}_\mu | n(p) \rangle = \bar{\psi}^\alpha(p') \Gamma_{\mu\alpha} u_n(p), \quad (22)$$

where  $\psi^\alpha$  is the spin-3/2 particle wave function and the vertex  $\Gamma_{\mu\alpha}$  is expressed in terms of the eight weak form factors  $C_{i=3,4,5,6}^{V,A}$  as

$$\begin{aligned} \Gamma_{\mu\alpha} = & \left[ \frac{g_{\mu\alpha} \not{q} - \gamma_\mu q_\alpha}{M} C_3^V + \frac{g_{\mu\alpha} p' \cdot q - p'_\mu q_\alpha}{M^2} C_4^V \right. \\ & + \frac{g_{\mu\alpha} p \cdot q - p_\mu q_\alpha}{M^2} C_5^V + \frac{q_\mu q_\alpha}{M^2} C_6^V \Big] \gamma_5 \\ & + \frac{g_{\mu\alpha} \not{q} - \gamma_\mu q_\alpha}{M} C_3^A + \frac{g_{\mu\alpha} p' \cdot q - p'_\mu q_\alpha}{M^2} C_4^A \\ & + g_{\mu\alpha} C_5^A + \frac{q_\mu q_\alpha}{M^2} C_6^A. \end{aligned} \quad (23)$$

By using the isospin invariance and the Wigner-Eckart theorem, we obtain another nucleon- $\Delta$  weak transition current as

$$\langle \Delta^{++} | \hat{J}_\mu | p \rangle = \sqrt{3} \langle \Delta^+ | \hat{J}_\mu | n \rangle. \quad (24)$$

From the CVC hypothesis,  $C_6^V = 0$  and the other vector form factors  $C_{i=3,4,5}^V$  are related to the electromagnetic form factors. We adopt the modified dipole parameterizations [14,15]:

$$\begin{aligned} C_3^V(q^2) &= \frac{C_3^V(0)}{(1 - \frac{q^2}{M_V^2})^2} \frac{1}{1 - \frac{q^2}{4M_V^2}}, \\ C_4^V(q^2) &= -\frac{M}{M_\Delta} C_3^V(q^2), \quad C_5^V(q^2) = 0, \end{aligned} \quad (25)$$

with  $C_3^V(0) = 2.05$  and  $M_V = 0.735$  GeV. For axial form factors, we use [14]

$$C_5^A(q^2) = \frac{C_5^A(0)}{(1 - \frac{q^2}{M_A^2})^2} \frac{1}{1 - \frac{q^2}{3M_A^2}}, \quad (26)$$

$$C_6^A(q^2) = \frac{M^2}{m_\pi^2 - q^2} C_5^A(q^2), \quad (27)$$

with  $C_3^V(0) = 2.05$  and  $M_A = 1.0$  GeV. For  $C_3^A$  and  $C_4^A$ ,  $C_3^A = 0$  and  $C_4^A = -\frac{1}{4}C_5^A$  give good agreements with the data [12]. As in the case of the  $F_p(q^2)$  of the QE process,  $C_6^A(q^2)$  has significant effects on the  $\tau$  production cross section and the  $\tau$  polarization [11].

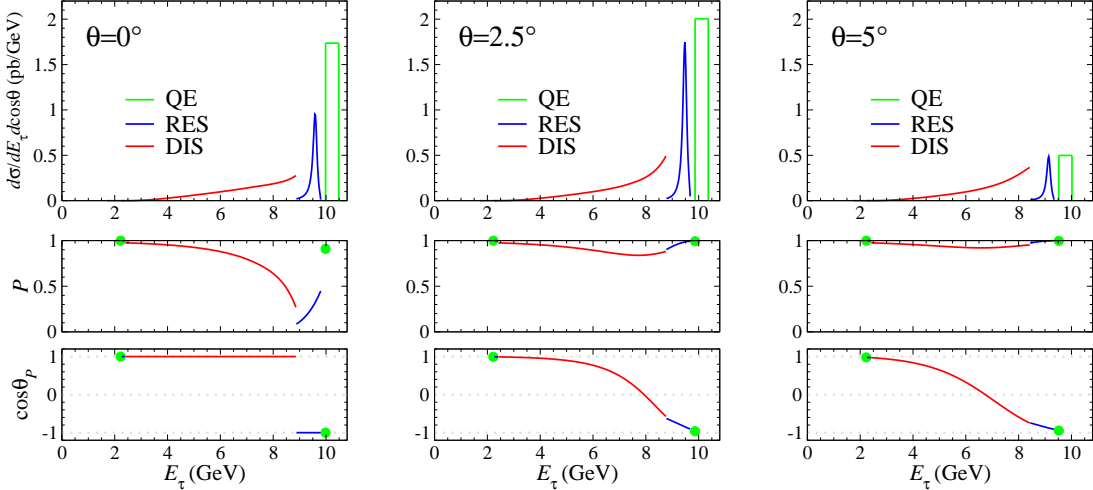


Figure 2. Production cross section and the  $\tau$  polarization of the process  $\nu_\tau N \rightarrow \tau^- X$  at  $E_\nu = 10$  GeV.  $E_\tau$  dependence of the differential cross section (top), the degree of polarization  $P$  (middle) and the polar component of the normalized polarization vector  $\cos \theta_P$  (bottom) are shown along the laboratory frame scattering angle  $\theta = 0^\circ$  (left),  $2.5^\circ$  (center) and  $5^\circ$  (right), respectively.

### 3.3. Deep inelastic scattering (DIS)

In the DIS region, the hadronic tensor is estimated by using the quark-parton model;

$$W_{\mu\nu}^{\text{DIS}}(p, q) = \sum_{q, \bar{q}} \int \frac{d\xi}{\xi} f_{q, \bar{q}}(\xi, Q^2) K_{\mu\nu}^{(q, \bar{q})}(p_q, q), \quad (28)$$

where  $p_q = \xi p$  is the four-momentum of the scattering quark,  $\xi$  is its momentum fraction, and  $f_{q, \bar{q}}$  are the parton distribution function(PDF)'s inside a nucleon. The quark tensor  $K_{\mu\nu}^{(q, \bar{q})}$  is

$$\begin{aligned} K_{\mu\nu}^{(q, \bar{q})}(p_q, q) = & \delta(2p_q \cdot q - Q^2 - m_{q'}^2) \\ & \times 2[-g_{\mu\nu}(p_q \cdot q) + 2p_{q\mu}p_{q\nu} \\ & + p_{q\mu}q_\nu + q_\mu p_{q\nu} \mp i\epsilon_{\mu\nu\alpha\beta}p_q^\alpha q^\beta]. \end{aligned} \quad (29)$$

The upper sign should be taken for quarks and the lower for antiquarks. We retain the final quark mass  $m_{q'}$  for the charm quark as  $m_c = 1.25$  GeV, but otherwise we set  $m_{q'} = 0$ . In the calculation, we used the MRST2002 [16] as the PDF's<sup>2</sup>.

### 4. POLARIZATION OF PRODUCED $\tau^-$

We show the spin polarization vector of  $\tau$  lepton produced by neutrino off isoscalar targets as a function of its energy  $E_\tau$  and the scattering angle  $\theta$  in the laboratory frame.

Figure 2 summarizes our results<sup>3</sup> for the  $\nu_\tau N \rightarrow \tau^- X$  process at  $E_\nu = 10$  GeV.

The top three figures show the double differential cross sections as a function of  $E_\tau$  at the scattering angle  $\theta = 0^\circ$  (left figures),  $5^\circ$  (center figures) and  $10^\circ$  (right figures). The area of the histogram for the QE process is normalized to the cross section. The QE and RES cross sections are large at forward scattering angles, and the DIS contribution become more significant at large scattering angles, though the cross section gets smaller.

A set of three middle figures give the degree of polarization  $P$ , and in the bottom three figures we show the polarization direction  $\cos \theta_P$  in Eq. (5). The produced  $\tau^-$  is almost fully polarized except at the very small scattering angle. As for

<sup>2</sup>We use naive extrapolation of the parton model calculation, even when  $Q^2 < Q_0^2$  ( $= 1.25$  GeV $^2$  in MRST2002)

<sup>3</sup>The Fortran code for our calculation of tau polarization is available on the web [17].

the angle of the polarization vector, the high energy  $\tau^-$  is almost left-handed ( $\cos\theta_P = -1$ ). On the other hand, the spin of low energy  $\tau^-$  turns around. The azimuthal angle  $\varphi_P$  takes  $\pi$  at all energies, which means that the spin vector points to the direction of the initial neutrino momentum axis.

In order to understand the above features, it is useful to consider the polarization of  $\tau^-$  in the center of mass (CM) frame of the scattering particles. Let us consider the DIS process in the  $\nu q$  CM frame, since the  $\nu q$  scattering is dominant in the  $\nu_\tau N \rightarrow \tau^- X$  process. In this frame, produced  $\tau^-$  is fully left-handed polarized at all scattering angles. This is because the initial  $\nu_\tau$  and  $q$  ( $d$  or  $s$  quarks) are both left-handed and hence angular momentum along the initial momentum direction is zero, while in the final state the produced  $u$  quark is left-handed and hence only the left-handed  $\tau^-$  is allowed by the angular momentum conservation. This selection rule is violated slightly when a charm quark is produced in the final state and because of gluon radiation at higher orders of QCD perturbation theory. The  $\tau^-$  polarization in the laboratory frame is then obtained by the Lorentz boost. In the QE and RES processes, situations are almost the same as in the DIS process. In the CM frame of  $\nu N$  collisions, the  $\tau^-$  lepton produced by the QE or RES process is almost left-handed at all angles, for the CM energy of  $\sqrt{2ME_\nu + M^2} \approx 4.4$  GeV for  $E_\nu = 10$  GeV, for our parametrizations of the transition form factors. High energy  $\tau^-$ 's in the laboratory frame have left-handed polarization because those  $\tau^-$ 's have forward scattering angles also in the CM frame. However, lower energy  $\tau^-$ 's in the laboratory frame tends to have right-handed polarization because they are produced at backward angles in the CM frame. At the zero scattering angle  $\theta = 0^\circ$  of the laboratory frame, the change in the  $\tau^-$  momentum direction occurs suddenly, and hence the transition from the left-handed  $\tau^-$  at high energies to the right-handed  $\tau^-$  at low energies is discontinuous.

## 5. CONCLUSION

The information on the polarization of  $\tau$  produced through the neutrino-nucleon scattering is essential to identify the  $\tau$  production signal since the decay particle distributions depend crucially on the  $\tau$  spin polarization. It is needed in long baseline neutrino oscillation experiments which should verify the large  $\nu_\mu \rightarrow \nu_\tau$  oscillation, and is also needed for the background estimation of  $\nu_\mu \rightarrow \nu_e$  appearance experiments which should measure the small mixing angle of  $\nu_e$ - $\nu_\mu$  oscillation.

In this report we presented the spin polarization of  $\tau^-$  produced in tau-neutrino nucleon scattering via charged currents. Quasi-elastic scattering (QE),  $\Delta$  resonance production (RES) and deep inelastic scattering (DIS) processes have been studied. The three subprocesses are distinguished by the hadronic invariant mass  $W$ .  $W = M (= m_N)$  gives QE,  $M + m_\pi < W < W_{\text{cut}}$  gives RES, and  $W > W_{\text{cut}}$  gives DIS. Here we set the kinematical boundary of RES and DIS process at  $W_{\text{cut}} = 1.6$  GeV.

The spin density matrix of  $\tau$  production has been defined and the  $\tau$  spin polarization vector has been defined and parametrized in the  $\tau$  rest frame whose polar-axis is taken along the momentum direction of  $\tau$  in the laboratory frame. The spin density matrix has been calculated for each subprocess by using the form factors for the QE and RES processes, and by using the parton distribution functions for the DIS process. We have shown the spin polarizations of  $\tau$  as function of the  $\tau$  energy and the scattering angle in the laboratory frame for  $\nu_\tau N \rightarrow \tau^- X$  process at  $E_\nu = 10$  GeV. We found that the produced  $\tau^-$  have high degree of polarization, but their spin directions deviate significantly from the massless limit predictions at low and moderate  $\tau$  energies. Qualitative feature of the predictions have been understood by considering the helicity amplitudes in the CM frame of the scattering particles and the effects of Lorentz boost from the CM frame to the laboratory frame.

Finally, we summarize our findings in Figure 3. In Figure 3, we show the polarization vector  $\vec{s}$  of  $\tau^-$  for the  $\nu_\tau N \rightarrow \tau^- X$  process at  $E_\nu = 10$  GeV

on the  $(p_\tau \cos \theta, p_\tau \sin \theta)$  plane, where  $p_\tau$  and  $\theta$  are the produced  $\tau$  momentum and the scattering angle in the laboratory frame. The length of each arrow gives the degree of polarization ( $0 \leq P \leq 1$ ) at each phase-space point and its orientation gives the spin direction in the  $\tau^-$  rest frame. The differential cross section is described as a contour map, where only the DIS cross section is plotted to avoid too much complexity. The outer line gives the kinematical boundary, along which the QE process occurs. Figure 3 is a more visual version of the information given in Figure 2.

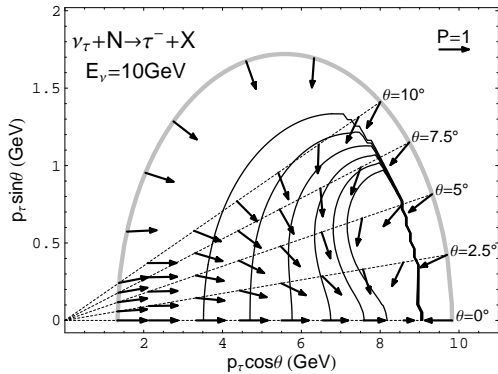


Figure 3. The contour map of the DIS cross section in the  $(p_\tau \cos \theta, p_\tau \sin \theta)$  plane for the  $\nu_\tau N \rightarrow \tau^- X$  process at  $E_\nu = 10$  GeV in the laboratory frame. The kinematical boundary is shown by the thick gray curve. The QE process contributes along the boundary, and the RES process contributes just inside of the boundary. The  $\tau^-$  polarization are shown by the arrows. The length of the arrows give the degree of polarization, and the direction of arrows give that of the  $\tau^-$  spin in the  $\tau^-$  rest frame. The size of the 100% polarization ( $P = 1$ ) arrow is shown as a reference. The arrows are shown along the laboratory scattering angles,  $\theta = 0^\circ, 2.5^\circ, 5^\circ, 7.5^\circ$ , and  $10^\circ$ , as well as along the kinematical boundary.

### Acknowledgements

K.M. and H.Y. are grateful to the organizers for the interesting and pleasant workshop and also

for giving us the opportunity to present this work. K.M. would like to thank T. Morii and M. Sakuda for encouragements. H.Y. would like to thank RIKEN BNL Research Center for the support of travel expense for this workshop.

### REFERENCES

1. ICARUS Collaboration home page, <http://pcnometh4.cern.ch/>.
2. OPERA Collaboration home page, <http://operaweb.web.cern.ch/>.
3. CNGS project home page, <http://proj-cngs.web.cern.ch/>.
4. K. Hagiwara, K. Mawatari, H. Yokoya, Nucl. Phys. B 668 (2003) 364 [arXiv: hep-ph/0305324].
5. K.S. Kuzmin, V.V. Lyubushkin, V.A. Naumov, hep-ph/0312107. They considered tau polarization with a covariant method.
6. K.M. Graczyk, hep-ph/0407283.
7. A. Bodek, U.K. Yang, Nucl. Phys. B (Proc. Suppl.) 112 (2002) 70.
8. C.H. Llewellyn Smith, Phys. Rep. 3 (1972) 261.
9. S. Eidelman et al. (Particle Data Group), Phys. Lett. B 592 (2004) 1.
10. V. Bernard, L. Elouadrhiri, U. Meissner, J. Phys. G 28 (2002) R1.
11. K. Hagiwara, K. Mawatari, H. Yokoya, Phys. Lett. B 591 (2004) 113 [arXiv: hep-ph/0403076].
12. P.A. Schreiner and F. Von Hippel, Nucl. Phys. B 58 (1973) 333.
13. S.K. Singh, M.J. Vicente Vacas, E. Oset, Phys. Lett. B 416 (1998) 23.
14. E.A. Paschos, J.Y. Yu, M. Sakuda, Phys. Rev. D 69 (2004) 014013.
15. M.G. Olsson, E.T. Osypowski, E.H. Monsay, Phys. Rev. D 17 (1978) 2938.
16. A.D. Martin, et al., Eur. Phys. J. C 23 (2002) 73.
17. An Open FORTRAN code for tau polarization in tau-neutrino nucleon scattering; <http://home.hiroshima-u.ac.jp/yokoya/taupol/>.